

1 **RNA sequencing analyses of gene expression by CRISPR/Cas9 knockout of**

2 **CLL-1 gene in acute myeloid leukemia cells**

3 Yanyu Wang^{*1}, Songfang Wu^{*2}, Jing Yang³, ShiLiang Wang³, Hong Xiong^{&1}, Shui-Jun

4 Li^{&2}

5 ¹Department of Hematology Fudan University Shanghai XuHui District hospital,

6 Shanghai, 200030, China;

7 ²Central laboratory, Fudan University Shanghai XuHui District hospital, Shanghai,

8 200030, China;

9 ³Cancer Institute, Middle Longhua Hospital, Shanghai University of Traditional

10 Chinese Medicine, Shanghai 200030, China;

11 ***Corresponding author**

12 *Yanyu Wang, Songfang, contributed equally to this work.

13 & to whom correspondence may be addressed. Email: xhxymzd666@163.com,

14 shuijunli@163.com,

15 Address: No. 966 Middle Huaihai Rd, XuHui District, Shanghai 200030, China,

16 Tel: +86-1231270810; Fax: +86-2164085875;

17 **Data Availability Statement**

18 The datasets used and/or analysed during the current study are available from the

19 corresponding author on reasonable request.

20

21 **Funding Statement**

22 The study was supported by XuHui district of ministry of health [SHXH201708].

23 **Conflict of Interest Disclosure**

24 All authors declare that they have no conflict of interest.

25

26 **Ethics Approval Statement**

27 Not applicable

28

29 **Patient Consent Statement**

30 Not applicable

31

32 **Permission to Reproduce Material from other Sources**

33 Not applicable.

34

35 **Clinical Trial Registration**

36 Not applicable

37

38 **Abstract**

39 CLL-1 has been revealed its potential role in acute myeloid leukemia (AML),
40 however, the underlying mechanisms remain unclear. CRISPR/Cas9 strategy was
41 employed to knock out CLL-1 gene in U937 cells and western-blot was used to
42 validate the success of knock out. CCK8 and Transwell assays were used to detect
43 cells viability and migration, respectively. RNA-sequencing was performed to profile
44 mRNA expression in CLL-1 gene knock-out and wide type U937 cells. A cutoff of
45 1.5-fold change and false discovery rate (FDR) <0.05 was used to screen differentially

46 expressed genes (DEGs), which were presented by volcano plots and hierarchical
47 cluster heatmap. Protein-protein interaction (PPI) network was constructed by String
48 database and Cytoscape software. Furthermore, hub genes were mined by CytoNCA
49 and MCODE, which were subjected to functional enrichment using R package.
50 Finally, the findings were validated using qRT-PCR and western-blot. The protein
51 level of CLL-1 was significantly lowered, and cell viability and migration were
52 suppressed in knock-out cells compared to wide type. Using RNA-sequencing and
53 bioinformatics analysis, 452 DEGs (179 up-regulated and 273 down-regulated) were
54 obtained, and several important hub genes (such as CCR2, FBXO21, UBB and
55 UBE2C) were filtered out, which were enriched in 132 GO terms and 36 KEGG
56 pathways such as chemokine signaling pathway and ubiquitin mediated proteolysis. A
57 total of 8 representative genes mRNA expressions were validated by qRT-PCR, and
58 the protein levels of 6 genes were confirmed by western-blot. CLL-1 gene might exert
59 its role in AML through modulating genes enriched in multiple functions such as
60 chemokine signaling and ubiquitination. Our results may give us new knowledge of
61 CLL-1 in AML and provide a basis for mining novel targets.

62

63 **Keywords:** CRISPR/Cas9; RNA sequencing; acute myeloid leukemia; CLL-1; gene
64 knockout.

65

66 **Introduction**

67 Acute myeloid leukemia (AML) is a disease of the bone marrow, a disorder of

68 hematopoietic stem cells due to genetic alterations in blood cell precursors resulting in
69 overproduction of neoplastic clonal myeloid stem cells (Pelcovits & Niroula,
70 2020). AML is the most common acute leukemia in adults and among the most lethal
71 (Kadia, Ravandi, Cortes, & Kantarjian, 2016). The median age at diagnosis of AML is
72 around 70 years, and approximately 3% of AML cases occur in children age 14 years
73 or younger (Tamamyian et al., 2017). The 2018 AML incidence estimates from SEER
74 are <1.23 per 100,000 in the <40-year-old population, 10.92 per 100,000 in the
75 ≥ 60 -year-old population and 20.89 per 100,000 in the ≥ 75 -year-old population in the
76 USA (Lin, Zhang, Yu, & Wu, 2021). However, there has been little progress in the
77 standard therapy for AML over the past four decades (Yang & Wang, 2018), further
78 understanding of the molecular heterogeneity and pathogenesis of AML is needed to
79 develop novel therapies.

80 With unprecedented advances in molecular genetics, a deeper insight into the biology
81 has opened doors to the development of therapeutic approaches in the hope of
82 achieving durable remissions and improving survival (Higgins & Shah, 2020). Besides,
83 recent advances in immunotherapy have generated substantial excitement for cancer
84 patients. Due to the immunosuppressive nature of AML, the activation of the immune
85 system through genetically engineered T-cell therapy presents a promising, curative
86 option for patients (Gill, 2019). C-type lectin-like receptors play a pivotal role in the
87 fight against infection and maintain homeostasis and self-tolerance by recognizing
88 damage associated and pathogen associated molecular patterns leading to regulation
89 of innate and adaptive immunity (Ma, Padmanabhan, Parmar, & Gong, 2019). C-type

90 lectin-like molecule-1(CLL-1 or CLEC12A) is a type-II transmembrane glycoprotein,
91 which belongs to the C-type lectin-like receptor family (J. Wang et al., 2018). It is
92 reported that CLEC12A/CLL-1 played an essential role in attenuating sterile
93 inflammation which is induced by uric acid crystal in a Syk-dependent pathway
94 (Neumann et al., 2014). In a collagen antibody-induced arthritis (CAIA) model,
95 *Clec12a*^{-/-} mice experienced more severe inflammation during CAIA due to the
96 over-activation of myeloid cells (Begun et al., 2015).

97 Intriguingly, CLEC12A has been found selectively present on leukemic stem cells
98 (LSCs) in AML but absent in normal HSCs (Leipold et al., 2018), which may be an
99 effective alternative target for AML with specificity against leukemic progenitor cells
100 and their progeny, while sparing normal myeloid precursor cells. Indeed,
101 mono-antibody therapy targeting CLL-1 has been revealed its potential efficacy
102 against AML cells and shown to be effective in reducing AML burden in xenograft
103 model (Lu et al., 2014). Researchers have developed and optimized CLL-1 CAR-T for
104 AML and showed efficient and specific anti-leukemia activity to AML cell lines and
105 primary blasts from AML patients, as well as in mouse model (Laborda et al., 2017;
106 Tashiro et al., 2017). Our previous study revealed that CLL-1 is a novel prognostic
107 predictor that could be exploited to supplement the current AML prognostic risk
108 stratification system, and potentially optimize the clinical management of AML (Y. Y.
109 Wang et al., 2017).However, the exact physiological function and underlying
110 mechanisms of CLL-1 in AML need to be elucidated.

111 In the present study, CRISPR/Cas9 was used to knock out CLL-1 gene in AML U937

112 cells, and high-throughput RNA sequencing was performed to profile the changes of
113 mRNA expression. The results will broaden our knowledge of CLL-1 gene's function
114 and provide novel therapeutic targets in AML.

115

116 **Methods**

117 ***Cell culture***

118 The AML cell line U937 was obtained from the American Type Culture Collection
119 (Rockville, MD, USA), and maintained at 37 °C, in the presence of 5% CO₂ and in a
120 humidified atmosphere. The cells were cultured in RPMI-1640 medium (Gibco
121 Technologies, Germany), supplemented with 10% fetal bovine serum (Moregate,
122 Australia) and 1% penicillin/streptomycin (10,000 U/ml and 10,000 µg/ml
123 respectively; Gibco/Life Technologies, Germany).

124 ***Knockout of CLL-1 gene using CRISPR/Cas9***

125 CLL-1 gene was knocked out by Bioray Laboratories Inc. (Shanghai, China) using the
126 CRISPR/Cas9 gene editing system according to manufacturer's instructions. In brief,
127 the primers including CLL-1 sgRNA1- forward (5'-CACCGGCTGGACGC
128 CATACTG AGA-3'), CLL-1 sgRNA1- reverse (5'- AAATCTCATGTATGGCGT
129 CCAGC-3'), CLL-1 sgRNA2- forward (5'-CACCGGATATAGCTCACGACATAAT
130 T-3') and CLL-1 sgRNA2-reverse (5'-AAACAATTATGTCGTGAGCTATATC-3')
131 were synthesized. Cloning of the sgRNA oligos was performed using lentiCRISPR V2
132 vector. The vector lentiCRISPR V2 was digested using BbsI restriction endonuclease.
133 The diluted sgRNAs were then ligated in the vector lentiCRISPR V2 with T4 DNA

134 ligase. The ligated vector was inserted into E.cloni® 10G electro-competent cells.
135 Plasmid construction was performed according to protocol and confirmed by
136 sequencing. The U937 cells were transfected with CLL-1 knock-out plasmid using
137 Lipofectamine 2000 for 48 h. The transfected cells were selected with puromycin
138 (3ug/ml) for seven days. Thereafter, single-cell cloning was performed in a 96-well
139 plate to grow single clones. After growth, western blot and sequencing were
140 performed to confirm knock-out of CCL-gene according to manufacturer's protocols.

141 ***Cell viability assays***

142 The CCK-8 assay (Dojindo Molecular Technologies, Gaithersburg, MD, USA) was
143 performed to evaluate cell viability according to manufacturer's instructions. Briefly,
144 cells were seeded into 96-well plates (5×10^4 cells/well) and cultured for 24h,48 h and
145 72h, respectively. Subsequently, 10 µl of CCK-8 solution was added to each well and
146 incubated at 37 °C for 1 h. The absorbances (Abs) at 450 nm were recorded using a
147 microplate reader (Bio-Rad, Hercules, CA, USA).

148 ***Cell migration assay***

149 Cell migration was assessed using Transwell chambers with 8 µm pore size membrane
150 inserts (BD Falcon™; BD Biosciences) according to previously described methods
151 (Han et al., 2018). Briefly, 2×10^5 cells were seeded into the upper chamber
152 supplemented with 100 µl serum-free medium, while 700 µL RPMI1640 containing
153 10% FBS was added to the lower chamber. After 12 hours' incubation (5% CO₂,
154 37°C), non-migrated cells in the upper chamber were removed and migrated cells in
155 the lower chamber were fixed with 4% paraformaldehyde and stained with 0.1%

156 crystal violet. Finally, cells were washed with PBS and counted using an inverted
157 microscope (Olympus Corporation) with ImageJ software. The experiments for each
158 group were repeated in triplicate.

159 ***RNA sequencing raw data acquisition***

160 CLL-1 gene knock-out (KO) and wide type (WT) U937 cells (n=3, each group) were
161 harvested and subjected to total RNA extraction using TRIzol reagent (Beyotime,
162 China). RNA quality was evaluated by an Agilent 2100 Bioanalyzer, and RNA
163 samples (n=3, each group) with RNA integrity number (RIN) more than 7 were used
164 for purification, library preparation, amplification and sequencing for 150bp paired
165 end reads using Illumina HiSeq 2500 platform according to manufacturer's
166 instructions.

167 ***RNA sequencing data analysis***

168 Before read mapping, clean reads were obtained from the raw reads by removing the
169 adaptor sequences and low-quality reads using FastQC software. The clean reads were
170 then aligned to Human genome (GRCh38, NCBI) using the Hisat2 (Kim, Langmead,
171 & Salzberg, 2015) and reconstructed by Cufflinks (Ghosh & Chan, 2016). HTseq was
172 used to calculate the expression of genes (Anders, Pyl, & Huber, 2015). The read
173 counts of each transcript were normalized to the length of the individual transcript and
174 to the total mapped read counts in each sample and expressed as FPKM (Fragments
175 Per Kilobase of exon per Million mapped reads). Differential expression analysis was
176 performed using DESeq2 with the threshold of 1.5-fold change ($|\log_2\text{fold change}$
177 $|\gt;0.58$) and false discovery rate (FDR) less than 0.05. The differential expressed

178 mRNAs between WT and KO U937 cells were presented with volcano plots and
179 hierarchical cluster heatmap using R software.

180 ***GO and KEGG pathway enrichment***

181 To reveal the function of the differential expressed genes between WT and KO U937
182 cells, gene ontology (GO) (including biological process, cellular component and
183 molecular function) and Kyoto Encyclopedia of Genes and Genomes (KEGG)
184 pathway analysis was performed using the Bioconductor package clusterProfiler.

185 ***Protein-protein interaction network and module analysis***

186 Protein-protein interaction (PPI) was screened using STRING (<https://string-db.org/>)
187 database with interaction score of 0.9 as the threshold, and the PPI network was
188 visualized by Cytoscape software. Furthermore, CytoNCA was used to screen hub
189 genes based on the nodes degree, and the candidate modules were obtained by
190 molecular complex detection (MCODE) with default parameters: degree cut-off = 2,
191 node score cut-off = 0.2, k -core = 2, and max depth = 100.

192 ***Real-Time qPCR***

193 Total RNA was extracted from WT and KO U937 cells using TRIzol reagent
194 (Beyotime,China). Real-time qPCR was performed according to previously described
195 methods (Zhu et al., 2019). Briefly, the cDNA was synthesized using the PrimeScript
196 RT reagent Kit (Yeasen, China) and amplified by real-time qPCR with an SYBR
197 Green Kit (Yeasen, China) on QuantStudio 12K Flex Real-Time PCR System. The
198 relative gene expression levels were determined using $2^{-\Delta\Delta Ct}$ method with GAPDH as
199 an internal control. All of the primers were synthesized by Biosune (Shanghai, China),

200 and the sequences of primers were shown in Table 1.

201 ***Western-blot***

202 WT and KO U937 cells were harvested and subjected to total protein extraction using
203 RIPA lysis. For each sample, 50 µg of protein was used for gel electrophoresis in
204 10-14% SDS-PAGE gels and transferred to PVDF membranes (Merck Millipore,
205 Billerica, MA, USA). After blocking in 5% defatted milk, the membranes were
206 incubated with primary antibodies of FBXO21, FBXO21, FBXO25, UBB, USP53,
207 UBE2C, UBE2E3, USP2, USP44 and B-Actin overnight at 4 °C. After incubation
208 with secondary antibodies, signals were detected using the ECL detection system
209 (Thermo Fisher Scientific) and analyzed by ImageJ software.

210 ***Statistical analysis***

211 The data are presented as the mean ± SD, and statistical analysis was performed using
212 SPSS software (version 22.0). Student's t-test was used to compare continuous
213 variables, and $P < 0.05$ were considered as statistically significant.

214

215 **Results**

216 ***Confirmation of CLL-1 gene knock-out***

217 CLL-1 gene knock-out was confirmed by western blotting (GAPDH serve as internal
218 control) to ensure the absence of CLL-1 protein expression. As shown in Figure 1, the
219 CLL-1 protein level was significantly lowered in CLL-1 gene knock out U937 cells
220 compared to wide type, which indicated the successful knock-out of CLL-1 gene.

221 ***CLL-1 gene knock-out reduced cells viability and migration***

222 To examine the effects of CLL-1 gene knock-out on U937 cells viability and
223 migration, CCK-8 and Transwell assays were performed, respectively. After CLL-1
224 gene knock-out, the cells viability was obviously reduced at the time-point of 24h,48h
225 and 72h(Figure 2A). Besides, the migrated cells in CLL-1 knock-out group were
226 significantly decreased compared to wide type group (Figure 2B). These results
227 indicated CLL-1 gene might play an important role in the cell viability and migration
228 of AML.

229 ***CLL-1 gene knock-out altered mRNA profile in U937 cells***

230 To explore the underlying mechanisms of CLL-1 affecting AML, RNA-seq was
231 performed to profile the mRNA expression in CLL-1 knock-out and wide type U937
232 cells. The differential gene analysis (Figure3 A & B) revealed that there were 452
233 differentially expressed genes (DEGs) in KO cells compared to WT cells. In addition,
234 we noticed that there were 179 up-regulated (including TRMT12, IL1B, CD86, etc.)
235 and 273 down-regulated mRNAs (including FBXO25, FBXO21, UBE2C, etc.) The
236 top 30 representative mRNAs were listed in Table 2, and 452 DEGs were listed in
237 Table S1.

238 ***Protein-protein interaction network analysis***

239 To reveal protein-protein interaction (PPI) among DEGs, 452 DEGs were imported to
240 String database to screen and visualized by Cytoscape software. A PPI network with
241 340 nodes and 904 edges was obtained (Figure 4). To obtain the hub genes in the PPI
242 network, CytoNCA was performed. As shown in Figure 5A, the top 30 genes with
243 higher degrees (>13) were filtered out, which included UBB, IL1B, CD86, etc.

244 Furthermore, MCODE was performed to explore the important modules in the PPI
245 network. As shown in Figure 5B, we obtained a module with the highest score (9.684),
246 which composed of 20 nodes (including FBXO21, UBB, UBE2C, etc.) and 92 edges.

247 ***GO and KEGG pathway functional enrichment***

248 To better understand the biological functions of the 20 DEGs involved in the
249 important module, functional enrichment was performed. We noticed that these DEGs
250 were enriched in 132 GO terms and 36 pathways, including ubiquitin mediated
251 proteolysis, chemokine signaling pathway, protein ubiquitination, etc. For example,
252 GNG7, ADCY1, CXCL8 and CCR2 were enriched in chemokine signaling pathway.
253 UBE2C and UBE2E3 were enriched in ubiquitin mediated proteolysis and genes
254 including SPSB1, ZBTB16, UBB, TRIM71, UBE2C, FBXO21, LMO7 and UBE2E3
255 were enriched in protein ubiquitination. The TOP 30 GO terms and KEGG pathways
256 were presented in Figure 6, and detailed information was listed in Table S2 and Table
257 S3.

258 ***Validation of RNA-sequence data by qRT-PCR and western-blot***

259 To validate our findings from RNA-sequence, a total of 8 genes (including FBXO21,
260 FBXO25, UBB, USP53, UBE2C, UBE2E3, USP2 and USP44) were selected to
261 perform qRT-PCR and western-blot experiments. The results of qRT-PCR and
262 RNA-sequence data of all the 8 genes were in good accordance (Figure 7A), and 6
263 genes (FBXO21, FBXO25, UBB, USP53, UBE2C and UBE2E3) expression were
264 further verified in the protein level. These results indicated the reliability of our
265 RNA-sequence analysis.

266

267 **Discussion**

268 In the present study, we aimed to explore the effects and underlying mechanisms of
269 CLL-1 gene in AML, RNA-sequencing was performed to profile mRNA expression in
270 CLL-1 gene knock-out and wide type U937 cells. We obtained numerous
271 differentially expressed mRNAs in CLL-1 gene knock-out cells, and filtered out a
272 batch of important genes which enriched in multiple GO terms and KEGG pathways.
273 It is reported that CLL-1 gene might be the most prominently differently expressed
274 surface markers in AML (Daga et al., 2019). We observed that the viability and
275 migration were reduced in CLL-1 gene knock-out U937 cells, which implicated the
276 important role of CLL-1 in AML. Using RNA-sequencing, we obtained a batch of
277 differentially expressed genes related to CLL-1 gene knock-out, which might account
278 for the underlying mechanisms of its role in AML. AML is a bone marrow disease in
279 which the leukemic cells show constitutive release of a wide range of CCL and CXCL
280 chemokines and express several chemokine receptors (Kittang, Hatfield, Sand,
281 Reikvam, & Bruserud, 2010). It is noticed that chemokine receptors may play an
282 important role in orchestrating the migration of cells and mediating the recruitment of
283 immune cells (Stone, Hayward, Huang, Z, & Sanchez, 2017). CC chemokine receptor
284 2 (CCR2) is the chemokine receptor, which has been found to be associated with
285 advanced cancer, metastasis, and relapse (Nagarsheth, Wicha, & Zou, 2017). It is
286 reported that tumor growth was reduced in CCR2^{-/-} mice compared to wild-type mice
287 (Huang et al., 2007). It was shown that CCR2 was almost exclusively expressed on

288 monocytoid AML in human samples (Cignetti et al., 2003). High expression of CCR2
289 was observed in AML cell lines and 65% of human AML samples, and the blockade
290 of CCL2/CCR2 axis inhibited cells transmigration and proliferation in AML
291 (Macanas-Pirard et al., 2017). These previous studies indicated that chemokine
292 receptor CCR2 might play an important role in AML. In the present study, we noticed
293 that CCR2 gene expression was significantly lowered in CLL-1 knock-out U937 cells,
294 which was partially consistent with previous studies and implicated that CLL-1 gene
295 might affect AML through CCR2 signaling. However, we did not observe the change
296 of CCR2 ligand, which needed further investigation. In addition, we also observed
297 several hub genes (such as GNG7, ADCY1 and CXCL8) enriched in chemokine
298 signaling pathway were altered, which suggested that CLL-1 gene might modulate
299 chemokine signaling in AML.

300 Besides, we noticed that a batch of important genes such as UBB, UBE2C, FBXO21,
301 USP53 and UBE2E3 were significantly changed in CLL-1 knock-out cells and
302 enriched in ubiquitination related GO terms and pathways, which indicated that
303 CLL-1 might regulate ubiquitination in AML. Ubiquitination is an essential
304 post-translational modification involved in protein stability, localization, interactions,
305 and activity, which influences cell apoptosis, cell survival, cell-cycle progression,
306 DNA repair and antigen presentation, and is implicated in multiple pathophysiological
307 states and diseases such as cancer, infections and hereditary disorders (van Wijk,
308 Fulda, Dikic, & Heilemann, 2019). Ubiquitination is mediated by the sequential action
309 of ubiquitin-activating enzyme, ubiquitin-conjugating enzyme and ubiquitin protein

310 ligase (Manasanch & Orłowski, 2017), and the abundance of cellular ubiquitin is
311 modulated by a family of multiple ubiquitin genes such as UBB and UBC (Haakonsen
312 & Rape, 2017). UBB has been implicated in many tumors including ovarian cancer,
313 gastric cancer, lung adenocarcinoma, etc (Deng, Huang, Wang, & Chen, 2020; Gong,
314 Lin, & Yuan, 2020; Scarpa et al., 2020). However, there is no report about UBB in
315 AML. Here, we reported that the expression of UBB mRNA and protein levels were
316 lowered in CLL-1 knock-out U937 cells, which indicated that UBB might play a role
317 in AML. It has been reported that UBE2C (an ubiquitin-conjugating enzyme)
318 participated in carcinogenesis by regulating the cell proliferation, apoptosis, and
319 transcriptional processes (Jin et al., 2019). UBE2C mRNA and/or protein levels were
320 aberrantly increased in many cancer types with poor clinical outcomes, and inhibition
321 of UBE2C suppressed proliferation, clone formation, and malignant transformation in
322 tumor cells (Xie, Powell, Yao, Wu, & Dong, 2014). Although little is known about
323 UBE2C in AML, it has been reported that UBE2C gene expression was increased in
324 aneuploid acute myeloid leukemia, which implicated the correlation of UBE2C with
325 AML (Simonetti et al., 2019). In addition, FBXO21 belongs to F-box proteins which
326 serves as the substrate-recognition subunit of a SKP1-CUL1-F-box protein
327 (SCF)-type ubiquitin ligase (Watanabe, Yumimoto, & Nakayama, 2015), and
328 ubiquitin-specific proteases 53 (USP53) belongs to the family of deubiquitinating
329 enzymes, which catalyze the reversible modification of target proteins with ubiquitin
330 and stabilize proteins (Fraile, Quesada, Rodriguez, Freije, & Lopez-Otin, 2012). It has
331 been reported that knockdown of USP53 in Siha cells downregulated damage-specific

332 DNA binding protein and caused G2/M cell cycle arrest and decreased the survival
333 rate of cells in response to radiation (Zhou, Yao, Wu, Chen, & Fan, 2020). However,
334 little has been reported about the role of FBXO21 and USP53 in AML. In the present
335 study, we noticed that the mRNA and protein levels of FBXO21 and USP53 were
336 significantly decreased after CLL-1 gene knock-out. Further investigations on these
337 genes enriched in ubiquitination related GO terms and pathways may provide novel
338 targets in AML.

339 Despite the significant findings in the present study, there are some limitations should
340 be noted. Although several important genes expression were validated in mRNA and
341 protein levels, our results were mainly based on RNA-sequencing and bioinformatics
342 analysis, which need further biological function investigation. Besides, our results
343 were obtained from AML cell models, which needed further animal models and
344 large-scale patient experiments to verify.

345 In conclusion, knock out of CLL-1 gene suppressed cell viability and migration in
346 AML cell line U937 cells, and the underlying mechanisms might be related to a batch
347 of important genes which were enriched in multiple functions such as chemokine
348 signaling and ubiquitination. Our results may give us new knowledge of CLL-1 in
349 AML and provide a basis for mining novel targets.

350

351 **Acknowledgements**

352 Not applicable.

353

354 **Reference**

- 355 Anders, S., Pyl, P. T., & Huber, W. (2015). HTSeq--a Python framework to work with
356 high-throughput sequencing data. *Bioinformatics*, *31*(2), 166-169.
357 doi:10.1093/bioinformatics/btu638
- 358 Begun, J., Lassen, K. G., Jijon, H. B., Baxt, L. A., Goel, G., Heath, R. J., . . . Xavier,
359 R. J. (2015). Integrated Genomics of Crohn's Disease Risk Variant Identifies a
360 Role for CLEC12A in Antibacterial Autophagy. *Cell Rep*, *11*(12), 1905-1918.
361 doi:10.1016/j.celrep.2015.05.045
- 362 Cignetti, A., Vallario, A., Roato, I., Circosta, P., Strola, G., Scielzo, C., . . . Ghia, P.
363 (2003). The characterization of chemokine production and chemokine receptor
364 expression reveals possible functional cross-talks in AML blasts with
365 monocytic differentiation. *Exp Hematol*, *31*(6), 495-503.
366 doi:10.1016/s0301-472x(03)00066-3
- 367 Daga, S., Rosenberger, A., Quehenberger, F., Krisper, N., Prietl, B., Reinisch, A., . . .
368 Wolfler, A. (2019). High GPR56 surface expression correlates with a leukemic
369 stem cell gene signature in CD34-positive AML. *Cancer Med*, *8*(4),
370 1771-1778. doi:10.1002/cam4.2053
- 371 Deng, H., Huang, Y., Wang, L., & Chen, M. (2020). High Expression of UBB, RAC1,
372 and ITGB1 Predicts Worse Prognosis among Nonsmoking Patients with Lung
373 Adenocarcinoma through Bioinformatics Analysis. *Biomed Res Int*, *2020*,
374 2071593. doi:10.1155/2020/2071593
- 375 Fraile, J. M., Quesada, V., Rodriguez, D., Freije, J. M., & Lopez-Otin, C. (2012).

- 376 Deubiquitinases in cancer: new functions and therapeutic options. *Oncogene*,
377 *31*(19), 2373-2388. doi:10.1038/onc.2011.443
- 378 Ghosh, S., & Chan, C. K. (2016). Analysis of RNA-Seq Data Using TopHat and
379 Cufflinks. *Methods Mol Biol*, *1374*, 339-361.
380 doi:10.1007/978-1-4939-3167-5_18
- 381 Gill, S. I. (2019). How close are we to CAR T-cell therapy for AML? *Best Pract Res*
382 *Clin Haematol*, *32*(4), 101104. doi:10.1016/j.beha.2019.101104
- 383 Gong, G., Lin, T., & Yuan, Y. (2020). Integrated analysis of gene expression and DNA
384 methylation profiles in ovarian cancer. *J Ovarian Res*, *13*(1), 30.
385 doi:10.1186/s13048-020-00632-9
- 386 Haakonsen, D. L., & Rape, M. (2017). Ubiquitin levels: the next target against
387 gynecological cancers? *J Clin Invest*, *127*(12), 4228-4230.
388 doi:10.1172/JCI98262
- 389 Han, H., Chen, W., Yang, J., Liang, X., Wang, Y., Li, Q., . . . Li, K. (2018). Inhibition
390 of cell proliferation and migration through nucleobase-modified
391 polyamidoamine-mediated p53 delivery. *Int J Nanomedicine*, *13*, 1297-1311.
392 doi:10.2147/IJN.S146917
- 393 Higgins, A., & Shah, M. V. (2020). Genetic and Genomic Landscape of Secondary
394 and Therapy-Related Acute Myeloid Leukemia. *Genes (Basel)*, *11*(7).
395 doi:10.3390/genes11070749
- 396 Huang, B., Lei, Z., Zhao, J., Gong, W., Liu, J., Chen, Z., . . . Feng, Z. H. (2007).
397 CCL2/CCR2 pathway mediates recruitment of myeloid suppressor cells to

- 398 cancers. *Cancer Lett*, 252(1), 86-92. doi:10.1016/j.canlet.2006.12.012
- 399 Jin, D., Guo, J., Wu, Y., Du, J., Wang, X., An, J., . . . Wang, W. (2019). UBE2C,
400 Directly Targeted by miR-548e-5p, Increases the Cellular Growth and Invasive
401 Abilities of Cancer Cells Interacting with the EMT Marker Protein Zinc Finger
402 E-box Binding Homeobox 1/2 in NSCLC. *Theranostics*, 9(7), 2036-2055.
403 doi:10.7150/thno.32738
- 404 Kadia, T. M., Ravandi, F., Cortes, J., & Kantarjian, H. (2016). New drugs in acute
405 myeloid leukemia. *Ann Oncol*, 27(5), 770-778. doi:10.1093/annonc/mdw015
- 406 Kim, D., Langmead, B., & Salzberg, S. L. (2015). HISAT: a fast spliced aligner with
407 low memory requirements. *Nat Methods*, 12(4), 357-360.
408 doi:10.1038/nmeth.3317
- 409 Kittang, A. O., Hatfield, K., Sand, K., Reikvam, H., & Bruserud, O. (2010). The
410 chemokine network in acute myelogenous leukemia: molecular mechanisms
411 involved in leukemogenesis and therapeutic implications. *Curr Top Microbiol*
412 *Immunol*, 341, 149-172. doi:10.1007/82_2010_25
- 413 Laborda, E., Mazagova, M., Shao, S., Wang, X., Quirino, H., Woods, A. K., . . . Young,
414 T. S. (2017). Development of A Chimeric Antigen Receptor Targeting C-Type
415 Lectin-Like Molecule-1 for Human Acute Myeloid Leukemia. *Int J Mol Sci*,
416 18(11). doi:10.3390/ijms18112259
- 417 Leipold, D. D., Figueroa, I., Masih, S., Latifi, B., Yip, V., Shen, B. Q., . . . Kamath, A.
418 V. (2018). Preclinical pharmacokinetics and pharmacodynamics of
419 DCLL9718A: An antibody-drug conjugate for the treatment of acute myeloid

- 420 leukemia. *MAbs*, 10(8), 1312-1321. doi:10.1080/19420862.2018.1517565
- 421 Lin, G., Zhang, Y., Yu, L., & Wu, D. (2021). Cytotoxic effect of CLL1 CART cell
422 immunotherapy with PD1 silencing on relapsed/refractory acute myeloid
423 leukemia. *Mol Med Rep*, 23(3), 1. doi:10.3892/mmr.2021.11847
- 424 Lu, H., Zhou, Q., Deshmukh, V., Phull, H., Ma, J., Tardif, V., . . . Schultz, P. G. (2014).
425 Targeting human C-type lectin-like molecule-1 (CLL1) with a bispecific
426 antibody for immunotherapy of acute myeloid leukemia. *Angew Chem Int Ed*
427 *Engl*, 53(37), 9841-9845. doi:10.1002/anie.201405353
- 428 Ma, H., Padmanabhan, I. S., Parmar, S., & Gong, Y. (2019). Targeting CLL-1 for
429 acute myeloid leukemia therapy. *J Hematol Oncol*, 12(1), 41.
430 doi:10.1186/s13045-019-0726-5
- 431 Macanas-Pirard, P., Quezada, T., Navarrete, L., Broekhuizen, R., Leisewitz, A., Nervi,
432 B., & Ramirez, P. A. (2017). The CCL2/CCR2 Axis Affects Transmigration
433 and Proliferation but Not Resistance to Chemotherapy of Acute Myeloid
434 Leukemia Cells. *PloS one*, 12(1), e0168888.
435 doi:10.1371/journal.pone.0168888
- 436 Manasanch, E. E., & Orlowski, R. Z. (2017). Proteasome inhibitors in cancer therapy.
437 *Nat Rev Clin Oncol*, 14(7), 417-433. doi:10.1038/nrclinonc.2016.206
- 438 Nagarsheth, N., Wicha, M. S., & Zou, W. (2017). Chemokines in the cancer
439 microenvironment and their relevance in cancer immunotherapy. *Nat Rev*
440 *Immunol*, 17(9), 559-572. doi:10.1038/nri.2017.49
- 441 Neumann, K., Castineiras-Vilarino, M., Hockendorf, U., Hanneschlager, N., Lemeer,

- 442 S., Kupka, D., . . . Ruland, J. (2014). Clec12a is an inhibitory receptor for uric
443 acid crystals that regulates inflammation in response to cell death. *Immunity*,
444 *40*(3), 389-399. doi:10.1016/j.immuni.2013.12.015
- 445 Pelcovits, A., & Niroula, R. (2020). Acute Myeloid Leukemia: A Review. *R I Med J*
446 *(2013)*, *103*(3), 38-40.
- 447 Scarpa, E. S., Tasini, F., Crinelli, R., Ceccarini, C., Magnani, M., & Bianchi, M.
448 (2020). The Ubiquitin Gene Expression Pattern and Sensitivity to UBB and
449 UBC Knockdown Differentiate Primary 23132/87 and Metastatic MKN45
450 Gastric Cancer Cells. *Int J Mol Sci*, *21*(15). doi:10.3390/ijms21155435
- 451 Simonetti, G., Padella, A., do Valle, I. F., Fontana, M. C., Fonzi, E., Bruno, S., . . .
452 Martinelli, G. (2019). Aneuploid acute myeloid leukemia exhibits a signature
453 of genomic alterations in the cell cycle and protein degradation machinery.
454 *Cancer*, *125*(5), 712-725. doi:10.1002/cncr.31837
- 455 Stone, M. J., Hayward, J. A., Huang, C., Z, E. H., & Sanchez, J. (2017). Mechanisms
456 of Regulation of the Chemokine-Receptor Network. *Int J Mol Sci*, *18*(2).
457 doi:10.3390/ijms18020342
- 458 Tamamyran, G., Kadia, T., Ravandi, F., Borthakur, G., Cortes, J., Jabbour, E., . . .
459 Konopleva, M. (2017). Frontline treatment of acute myeloid leukemia in
460 adults. *Crit Rev Oncol Hematol*, *110*, 20-34.
461 doi:10.1016/j.critrevonc.2016.12.004
- 462 Tashiro, H., Sauer, T., Shum, T., Parikh, K., Mamonkin, M., Omer, B., . . . Brenner, M.
463 K. (2017). Treatment of Acute Myeloid Leukemia with T Cells Expressing

- 464 Chimeric Antigen Receptors Directed to C-type Lectin-like Molecule 1. *Mol*
465 *Theor*, 25(9), 2202-2213. doi:10.1016/j.ymthe.2017.05.024
- 466 van Wijk, S. J., Fulda, S., Dikic, I., & Heilemann, M. (2019). Visualizing
467 ubiquitination in mammalian cells. *EMBO Rep*, 20(2).
468 doi:10.15252/embr.201846520
- 469 Wang, J., Chen, S., Xiao, W., Li, W., Wang, L., Yang, S., . . . Zhou, P. (2018). CAR-T
470 cells targeting CLL-1 as an approach to treat acute myeloid leukemia. *J*
471 *Hematol Oncol*, 11(1), 7. doi:10.1186/s13045-017-0553-5
- 472 Wang, Y. Y., Chen, W. L., Weng, X. Q., Sheng, Y., Wu, J., Hao, J., . . . Wang, J. (2017).
473 Low CLL-1 Expression Is a Novel Adverse Predictor in 123 Patients with De
474 Novo CD34(+) Acute Myeloid Leukemia. *Stem Cells Dev*, 26(20), 1460-1467.
475 doi:10.1089/scd.2016.0310
- 476 Watanabe, K., Yumimoto, K., & Nakayama, K. I. (2015). FBXO21 mediates the
477 ubiquitylation and proteasomal degradation of EID1. *Genes Cells*, 20(8),
478 667-674. doi:10.1111/gtc.12260
- 479 Xie, C., Powell, C., Yao, M., Wu, J., & Dong, Q. (2014). Ubiquitin-conjugating
480 enzyme E2C: a potential cancer biomarker. *Int J Biochem Cell Biol*, 47,
481 113-117. doi:10.1016/j.biocel.2013.11.023
- 482 Yang, X., & Wang, J. (2018). Precision therapy for acute myeloid leukemia. *J*
483 *Hematol Oncol*, 11(1), 3. doi:10.1186/s13045-017-0543-7
- 484 Zhou, Q., Yao, X., Wu, C., Chen, S., & Fan, D. (2020). Knockdown of
485 Ubiquitin-Specific Protease 53 Enhances the Radiosensitivity of Human

486 Cervical Squamous Cell Carcinoma by Regulating DNA Damage-Binding

487 Protein 2. *Technol Cancer Res Treat*, 19, 1533033820929792.

488 doi:10.1177/1533033820929792

489 Zhu, K. P., Zhang, C. L., Ma, X. L., Hu, J. P., Cai, T., & Zhang, L. (2019). Analyzing

490 the Interactions of mRNAs and ncRNAs to Predict Competing Endogenous

491 RNA Networks in Osteosarcoma Chemo-Resistance. *Mol Ther*, 27(3), 518-530.

492 doi:10.1016/j.ymthe.2019.01.001

493

494 **Figure legends**

495 Figure 1. Western-blot analysis of CLL-1 expression in knock-out and wide type

496 U937 cells.

497 Figure 2. CCK8 and Transwell assays in CLL-1 knock-out and wide type U937 cells.

498 A. CCK8 assay, B. Transwell assay.

499 Figure 3. Volcano plots and hierarchical cluster analysis. A. Volcano plots, blue dots

500 represent down-regulated mRNAs, grey dots represent no significant changed

501 mRNAs, red dots represent up-regulated mRNAs. B. Heatmap of hierarchical cluster,

502 red colors indicate up-regulated and green colors indicate down-regulated.

503 Figure 4. PPI network of 452 DEGs. PPI network with 340 nodes and 904 edges, and

504 blue nodes indicate DEGs and edges indicate interactions.

505 Figure 5. Subnetworks of hub genes and an important module. A. Subnetwork of the

506 top 30 hub genes with higher degrees (>13). B. Subnetwork of an important module

507 with the highest score (9.684). Blue nodes indicate DEGs and edges indicate

508 interactions.

509 Figure 6. Top 30 GO terms and KEGG pathways. A. Top 30 GO terms, B. Top 30

510 KEGG pathways.

511 Figure 7. Validation by qRT-PCR and western-blot. A. The mRNA levels of 8 genes

512 were validated by qRT-PCR, the red line represents RNA sequence data and green line

513 represents qRT-PCR data. B. The protein levels of 8 genes were validated by

514 western-blot.

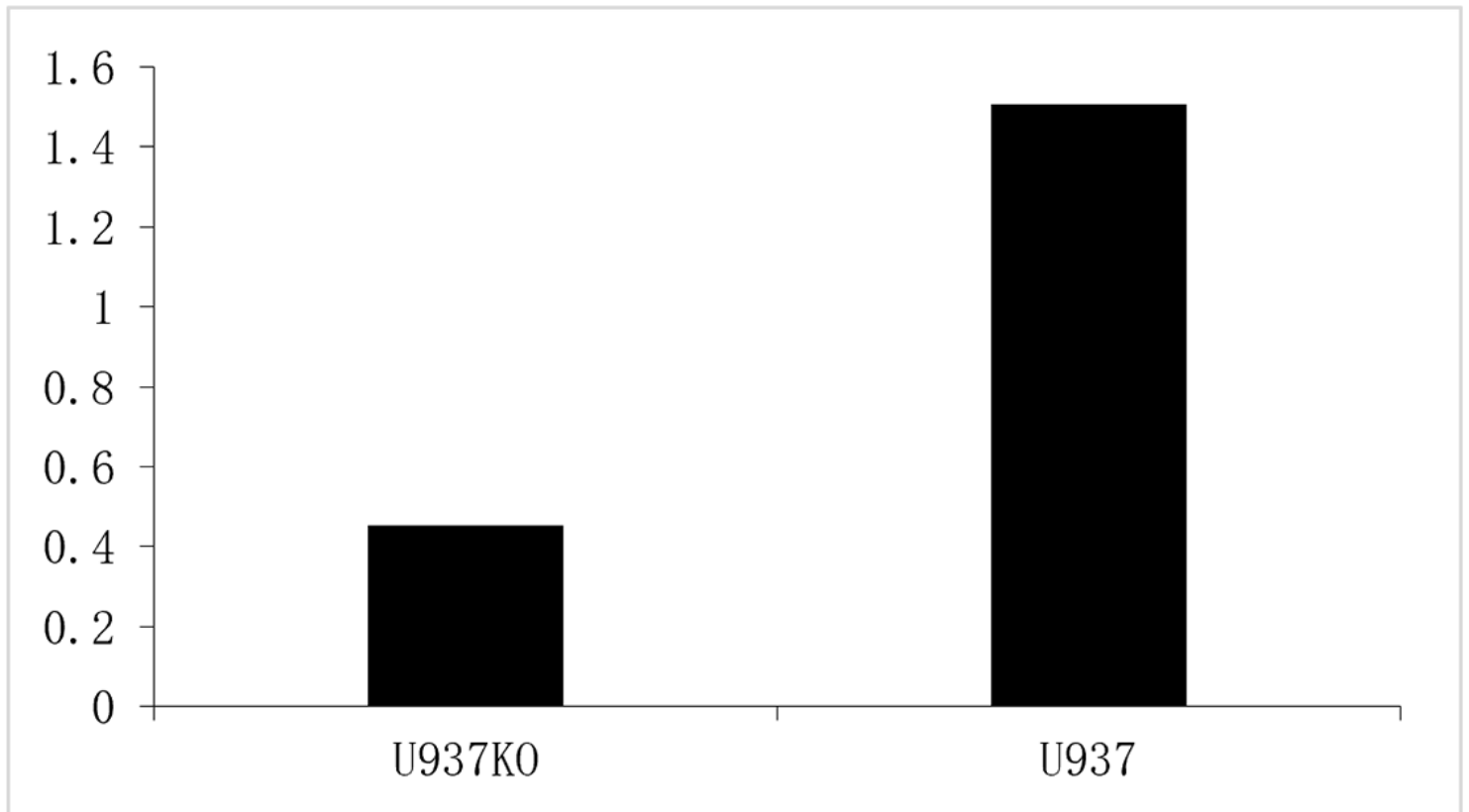
515

516 **Supporting Information**

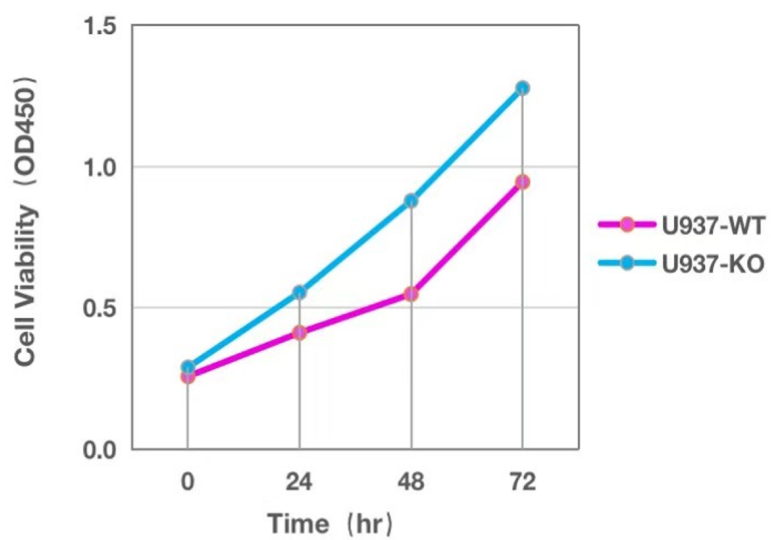
517 Table S1: WSF-KO_vs_WSF-WT.log2FC0.585.FDR0.05.Diff.mRNA&circRNA

518 Table S2: Negative_Analysis_miRNA_mRNA.GO-Analysis

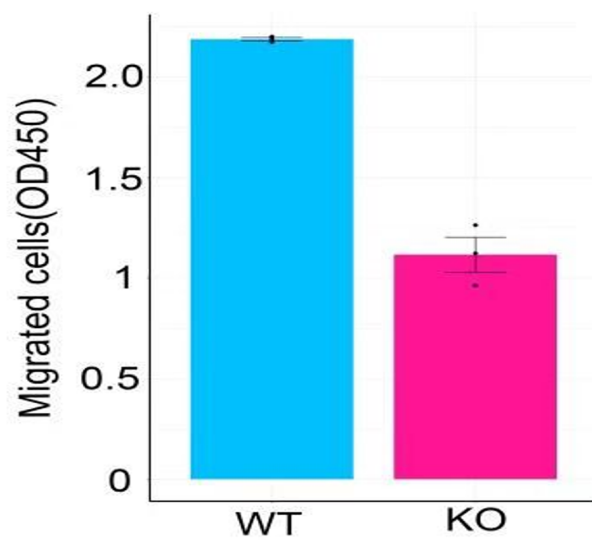
519 Table S3: Pathway Analysis Result

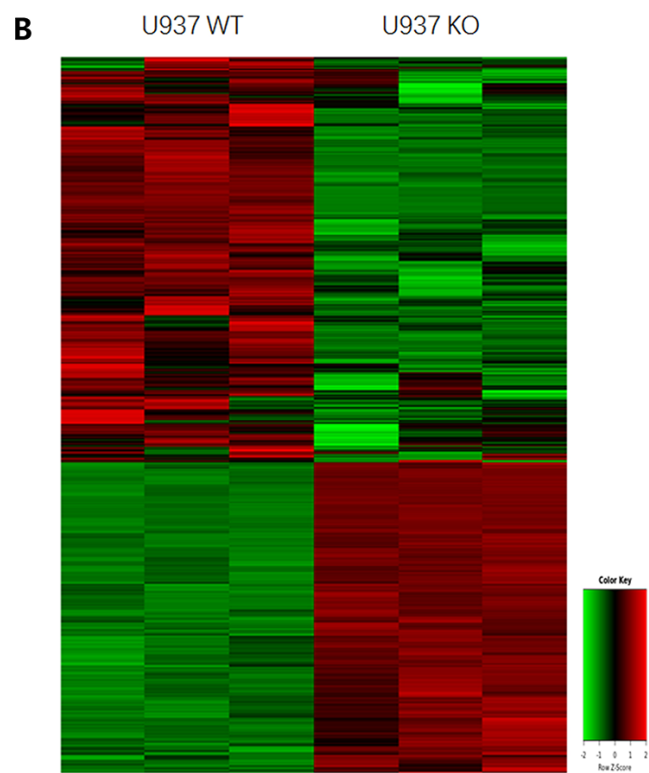
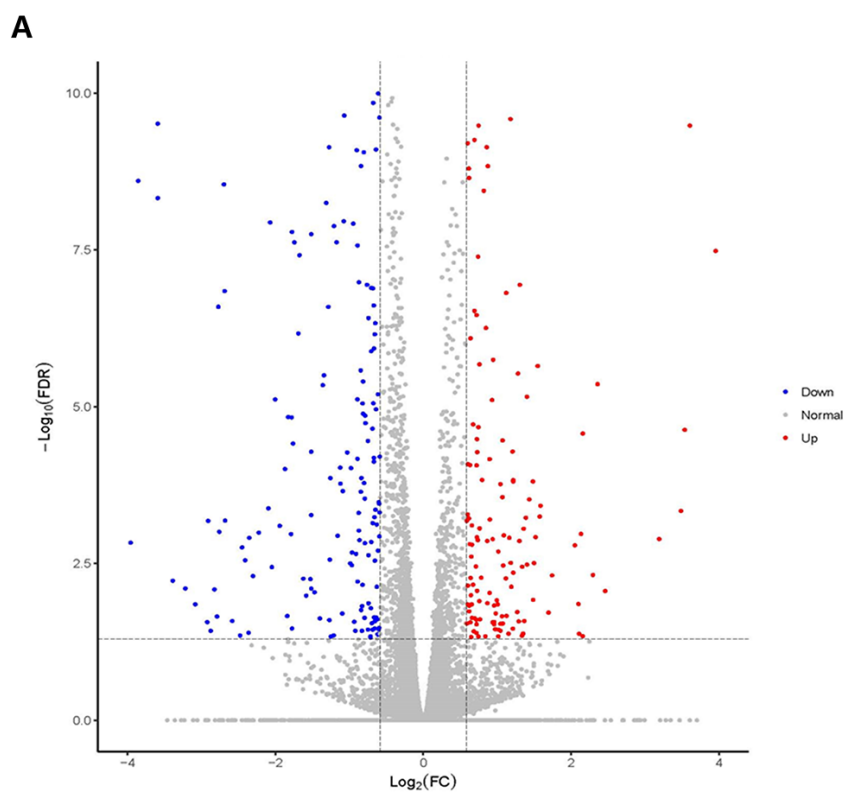


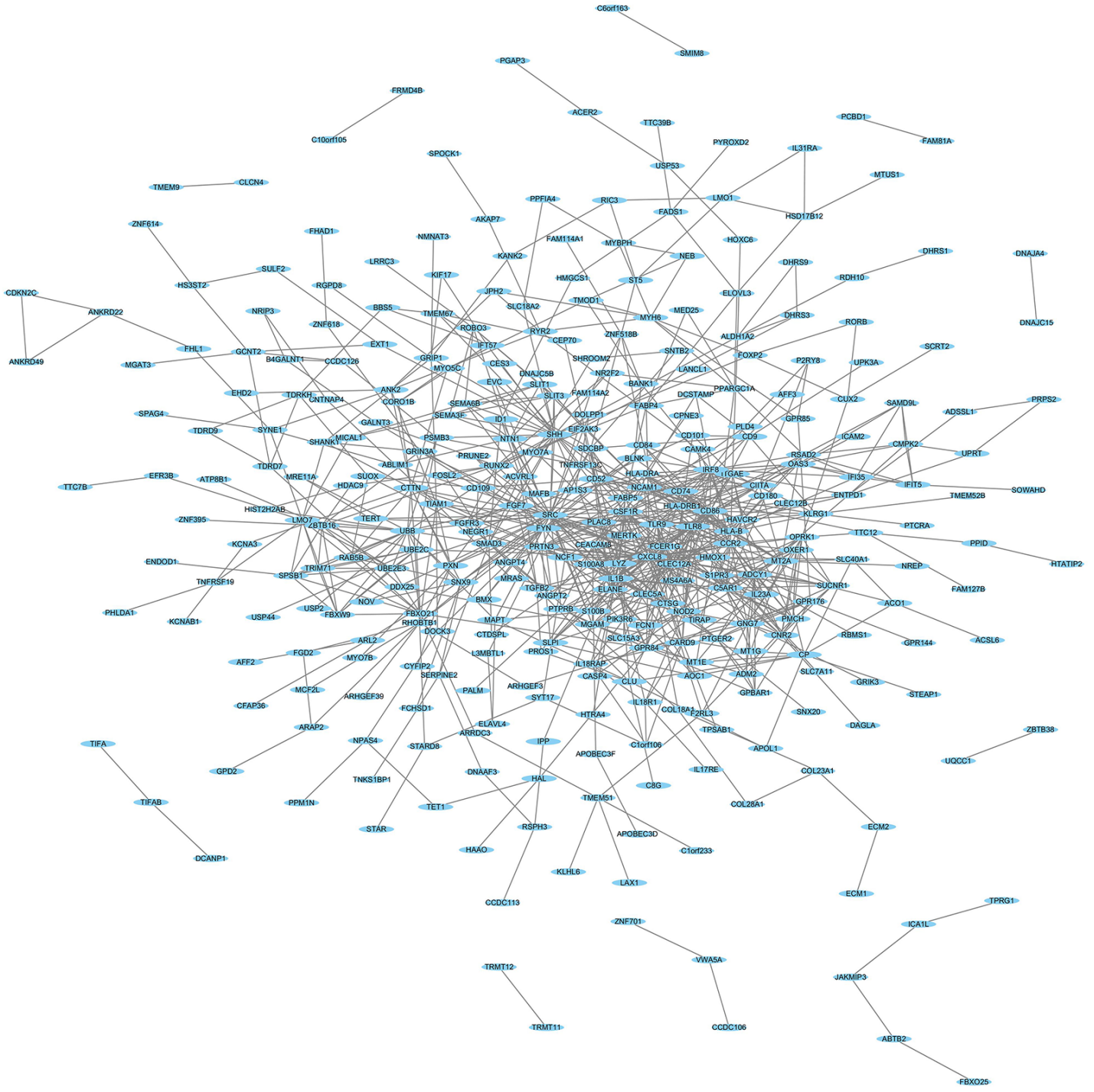
A



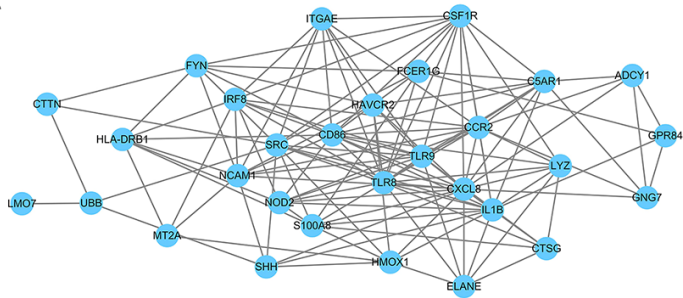
B



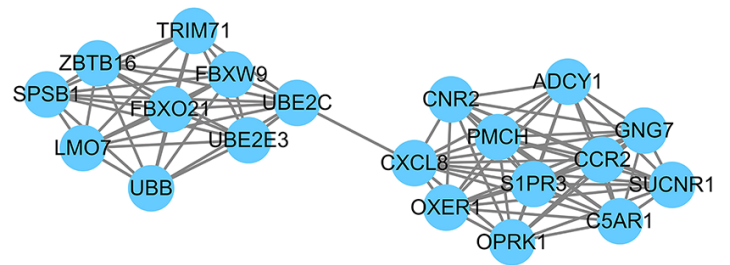




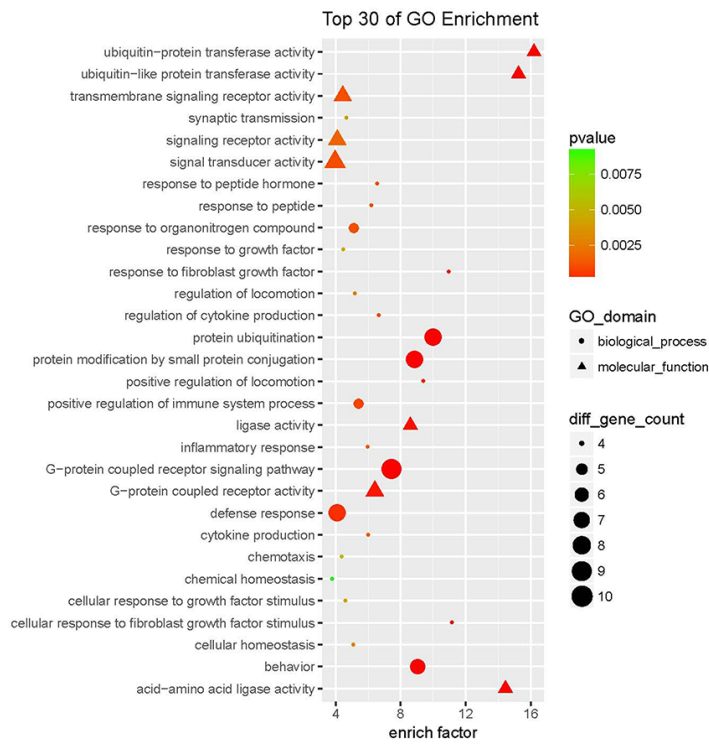
A



B



A



B

